Differences in the Intracellular Distribution of Acid-Sensitive Doxorubicin-Protein Conjugates in Comparison to Free and Liposomal Formulated Doxorubicin as shown by Confocal Microscopy

Ulrich Beyer,[1] Barbara Rothen-Rutishauser,[2] Clemens Unger,[3] Heidi Wunderli-Allenspach,[2] and Felix Kratz[3,4]

Received September 19, 2000; accepted October 2, 2000

Purpose. To investigate differences in the cellular uptake and intracellular distribution of protein-bound doxorubicin in comparison to free doxorubicin and a liposomal formulation (CAELYX®)

Methods. LXFL 529 lung carcinoma cells were incubated with an acid-sensitive transferrin and albumin conjugate of doxorubicin, a stable albumin doxorubicin conjugate, and free and liposomal doxorubicin for up to 24 h. The uptake of doxorubicin was detected with confocal laser scanning microscopy (CLSM). To investigate the intracellular localization of the anticancer drug, lysosomes, Golgi apparatus, and mitochondria were also stained by various organelle-specific fluorescent markers. *In vitro* efficacy of the doxorubicin derivatives was examined with the BrdU incorporation assay.

Results. The acid-sensitive albumin and transferrin doxorubicin conjugates showed enhanced cytotoxicity in comparison to liposomal doxorubicin, whereas the stable albumin-doxorubicin conjugate showed only marginal activity. Of all compounds tested, doxorubicin showed the highest cytotoxicity. CLSM studies with specific markers for lysosomes, mitochondria, and the Golgi apparatus demonstrated that protein-bound doxorubicin or liberated doxorubicin was accumulated in the mitochondria and Golgi compartments, but not in the lysosomes after 24 h. Free doxorubicin showed a time-dependent intracellular shift from the nucleus to the mitochondria and Golgi apparatus. Fluorescence resulting from incubation with CAELYX was primarily detected in the nucleus.

Conclusions. Our results indicate that other organelles in addition to the cell nucleus are important sites of accumulation and interaction for protein-bound doxorubicin or intracellularly released doxorubicin as well as for free doxorubicin.

KEY WORDS: doxorubicin; drug protein conjugates; CAELYX®; confocal laser scanning microscopy; organelle-specific markers; intracellular distribution.

INTRODUCTION

Coupling anticancer drugs to macromolecules (1) or incorporating them into liposomes (2) is a promising strategy of improving the selectivity of these agents for tumor tissue. The rationale for this drug delivery strategy is based on the observation that liposomes or polymers can accumulate in solid tumors due to an enhanced permeability of tumor blood vessels for circulating macromolecules (3).

For this reason, we recently synthesized a number of albumin and transferrin conjugates with the clinically widely used antineoplastic agent doxorubicin, which is well established in the treatment of leukemia, breast carcinoma, and other solid tumors (4,5). As shown in Fig. 1, doxorubicin maleimide derivatives were bound to albumin or transferrin, which contain either a stable amide bond at the 3′-amino position of the anthracycline (abbreviated A-DOXO-MBS) or an acid-sensitive carboxylic hydrazone bond at the 13-keto position (abbreviated A-DOXO-HYD, T-DOXO-HYD). The acid-sensitive link between drug and protein was designed to allow the drug to be released intracellularly in acidic endosomal or lysosomal compartments after cellular uptake of the conjugate by the tumor cell (6).

In vitro studies with these conjugates and free doxorubicin in several human tumor cell lines have shown that the acid-sensitive protein conjugates A-DOXO-HYD and T-DOXO-HYD were promising candidates for further biological assessment, whereas the conjugate in which the drug was bound through a stable amide bond to albumin (A-DOXO-MBS) showed no or only marginal inhibitory effects (4,5). Subsequent *in vivo* studies in tumor-bearing animal models demonstrated superior therapeutic effects for the acid-sensitive conjugate A-DOXO-HYD when compared to free doxorubicin at equitoxic dose (7,8); in contrast, A-DOXO-MBS showed no antitumor efficacy (8).

Note that first fluorescence and confocal laser scanning microscopy (CLSM) studies, which were recently published by our group, showed significant differences in the intracellular distribution of free doxorubicin and the doxorubicin of our transferrin conjugates (4): whereas the unbound drug was primarily detected in the nucleus after 24 h, most of the protein-bound doxorubicin or intracellularly released doxorubicin was localized in the cytoplasm. This fact is remarkable because of the observation that the *in vitro* efficacy of the acid-sensitive transferrin conjugate was similar to that of free doxorubicin (4).

On the basis of these observations, we wanted to obtain a more detailed picture of the intracellular distribution of protein doxorubicin conjugates in comparison to the free drug and a liposomal formulation of doxorubicin (CAELYX®). CAELYX is a pegylated liposomal formulation of doxorubicin which shows superior activity in several preclinical animal tumor models when compared to free doxorubicin (9). In addition to approval for the treatment of Kaposi's sarcoma, it has recently been approved for the second-line treatment of ovarian cancer in the United States (10).

For our studies, CLSM is particularly suitable because this technique allows a significant improvement in axial (z) as well as in lateral resolution in comparison to conventional fluorescence microscopy (11,12). In addition, fluorescent drugs as well as fluorescent markers for staining various compartments of living cells can be detected simultaneously and their colocalization can be analyzed using a suitable digital imaging software (13).

In the present work, we compared the cellular uptake and the intracellular distribution of the doxorubicin protein conjugates A-DOXO-HYD, T-DOXO-HYD, and A-DOXO-

[1] Present address: medac GmbH, Theaterstrasse 6, 22880 Wedel, Germany.

[2] Biopharmacy, Department of Applied BioSciences, Winterthurerstrasse 190, CH-8057 Zuerich, Switzerland.

[3] Tumor Biology Center, Department of Medical Oncology, Clinical Research, Breisacher Straße 117, D-79106 Freiburg, Germany.

[4] To whom correspondence should be addressed. (e-mail: felix@tumorbio.uni-freiburg.de)

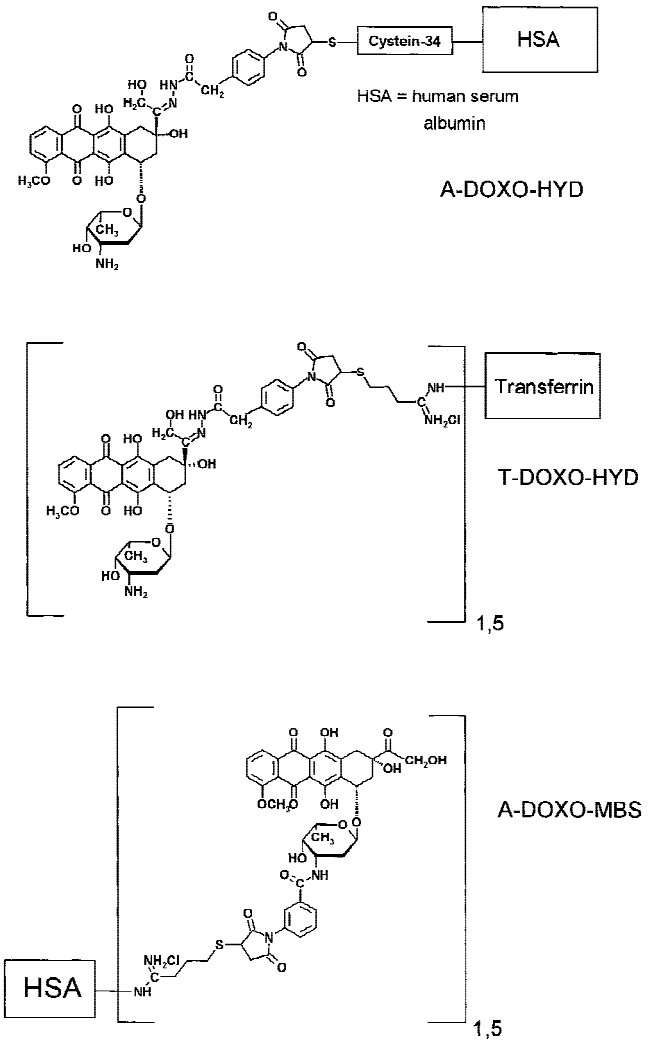

Fig. 1. Structures of the albumin-doxorubicin conjugates A-DOXO-MBS and A-DOXO-HYD and the transferrin-doxorubicin conjugate T-DOXO-HYD.

MBS of free doxorubicin and of CAELYX in lung carcinoma cells using CLSM. In particular, double labeling experiments in living cells with specific markers for lysosomes, mitochondria, and the Golgi apparatus were performed. In addition, the relationships between in vitro efficacy, stability, intracellular accumulation, and localization of the different doxorubicin derivatives are discussed.

MATERIALS AND METHODS

Doxorubicin Derivatives

The albumin and transferrin conjugates of doxorubicin were synthesized as previously described and used as a 300 μM stock solution in buffer (0.15 M NaCl, 0.004 M sodium phosphate, pH 7.4) (4,5). The precise characterization of the albumin doxorubicin conjugate A-DOXO-HYD, in which the doxorubicin maleimide spacer is bound to the cysteine-34 position of albumin, through electron spray mass spectrometry has been recently reported by us (14). The doxorubicin-protein conjugates contained approximately 1–2% of free doxorubicin and/or free doxorubicin spacer as shown by HPLC (size-exclusion HPLC BioSil SEC250 from Biorad, Germany, and reversed-phase HPLC on a C-18 SYMMETRY® from Waters, Germany) at $\lambda = 495$ nm and with the aid of fluorescence detection. These noncovalently bound forms of doxorubicin presumably bind to high-affinity binding sites on the respective protein and are difficult to remove even by repeated gel filtration over Sephadex® G-25. Doxorubicin × HCl was a gift from Pharmacia & Upjohn (Erlangen, Germany) and used as a 300 μM stock solution in isotonic saline. CAELYX was a gift from Essex Pharma (Munich, Germany) and has a liposome diameter of approximately 100 nm. The bilayer membrane consists of *N*-(carbonyl-methoxypolyethylene glycol 2000)-1,2-distearoyl-*sn*-glycero-3-phospaethanolamine sodium salt (3.19 mg/ml), fully hydrogenated soy 3-*sn*-phosphatidylcholine (9.58 mg/ml), and cholesterol (3.19 mg/ml); doxorubicin content was 2 mg/ml. According to consumer product information for CAELYX, greater than 90% of doxorubicin is encapsulated in the STEALTH® liposome. In the samples made available to us by Essex Pharma, Germany, we were unable to detect any free doxorubicin when CAELYX was gel filtrated over Sephadex G-25, however. CAELYX was diluted with phosphate-buffered saline (PBS) (0.008 M Na_2PO_4, 0.002 M KH_2PO_4, 0.13 M NaCl, pH 7.4) to a concentration of 300 μM immediately before use.

Fluorescence Spectra

Fluorescence spectra were recorded with a Perkin-Elmer LS50B spectrofluorimeter. Fluorescence was excited at 479 nm (excitation and emission slide widths were 5 and 20 nm, respectively; spectra were recorded from 500 to 750 nm). Doxorubicin or doxorubicin formulations were diluted with buffer (0.004 M sodium phosphate, 0.15 M NaCl, pH 7.4) to a concentration of 3.0 μM and fluorescence spectra were recorded at room temperature. For incubation studies with calf thymus DNA (from Sigma, Germany), DNA was added to a final concentration of $r \sim 0.01$ (0.6 mg/ml), where r is the ratio between the molar concentration of doxorubicin and the DNA base pairs. Fluorescence spectra were recorded after the samples were incubated with DNA for 5 min.

Cell Culture

LXFL 529 cells were grown as monolayer cultures in cell culture flasks (Greiner Labortechnik, Frickenhausen, Germany) in RPMI 1640 culture medium with phenol red supplemented with 10% heat-inactivated FCS, 100 μg/ml glutamine, 100 U/ml penicillin, and 100 μg/ml streptomycin. Cell culture media, supplements, and fetal calf serum (FCS) were purchased from Boehringer Ingelheim Bioproducts, Germany.

LXFL 529 human lung carcinoma cells were cultured at 37°C in a humidified atmosphere of 95% air and 5% carbon dioxide at 37°C. Media were routinely changed every 3 days. For subculture or experiments, cells growing as monolayer cultures were released from the tissue flasks by treatment with 0.05% trypsine/ethylenediaminetetraacetic acid (EDTA), and viability was monitored using the cell analyzer system Casy 1 from Schärfe Systems (Reutlingen, Germany). For the experiments, cells were used during the logarithmic growth phase.

BrdU-Incorporation Assay

The 5-bromo-2′-deoxyuridine cell proliferation kit (cat. no. 1647229) was obtained from Boehringer Mannheim (Mannheim, Germany). To determine the index of DNA synthesis, BrdU was measured according to the instructions of the manufacturer. Briefly, 1.0–1.2 × 10^4 cells/cm^2 were plated in each well of a 96-well tissue culture plate. Medium supplemented with 10% FCS was added and cells were allowed to adhere for 24 h. Subsequently, cells were preincubated with various drug concentrations for 20 h and were then labeled by adding 10 mM BrdU to each well. Cultures were incubated in the presence of BrdU for 4 h. After this period, cells were fixed with FixDenat solution at room temperature (RT) for 30 min, washed three times with washing solution at RT, and incubated with a monoclonal anti-BrdU-peroxidase Fab fragment (diluted 1:10000 with PBS) for 90 min at room temperature (RT). DNA was then washed three times with washing solution at RT and incorporated BrdU was visualized by adding 100 μl of the peroxidase substrate BM blue. After an incubation time of 10 min, the extinction of the samples was quantified with an ELISA reader (Dynatech Laboratories Inc., Sullyfield, U.K.) at a wavelength of 405 nm and set as the index of DNA synthesis. Four separate cultures were determined per concentration. Results are shown as means ± SD (n = 3); similar results were obtained in an additional separate experiment.

Confocal Microscopy

A Zeiss LSM 410 inverted microscope was used (lasers: HeNe 543 nm, Ar 488 nm, and Ar UV 364 nm). Optical sections at intervals of 0.3 μm were taken with a 63×/1.4 Plan-Apochromat objective.

Image processing was performed on a Silicon Graphics O2 workstation using IMARIS, a three-dimensional (3D) multichannel image processing software for confocal microscopic images (Bitplane AG, Zurich, Switzerland). Colocalization analyses were carried out using the "colocalization" software from Bitplane AG. The instrument adjustments for obtaining CLSM images were kept constant to allow image studies with the drug formulations to be compared with one another.

The CLSM experiments were performed in the following manner: After subcultivation, cells were resuspended in medium to a final concentration of approximately 2 × 10^4 cells/cm^2 and allowed to adhere on sterile ChamberSlides (NUNC, Denmark) with a thin glass bottom for 24 h. Cells were incubated with final drug concentrations of 1.0 μM (free doxorubicin) or 2.0 μM (all other substances) for 4 and 24 h, respectively. Subsequently, the nuclei of the cells were stained by incubation with Hoechst 33342 (final concentration: 1.76 μM; Molecular Probes, Eugene, Oregon) for 15 min. The medium was removed, the cells were washed twice with prewarmed medium, and the chamber slides with the medium-covered cells were transferred to the confocal microscope. Optical sections (40 layers, thickness: 0.3 μm) were taken at 488 nm (doxorubicin) and 364 nm (Hoechst 33342). In the next step, the cells were incubated for 15 min with the respective organelle-specific marker in prewarmed medium (final concentrations: 75 nM LysoTracker Red [L-7528] for lysosomes, 75 nM MitoTracker Red [M-7513] for mitochondria, 1.0 μM BODIPY® TR ceramide [D-7540] for the Golgi apparatus; all markers were purchased from Molecular Probes, Eugene Oregon). The medium was removed, and the cells were washed twice with PBS and then covered with PBS. Optical sections (40 layers, thickness: 0.3 μm) were taken at 543 nm (LysoTracker Red, MitoTracker Red, BODIPY TR ceramide) and 364 nm (Hoechst 33342). 3D visualization of the cell stacks was performed using IMARIS. The correct location of the cells was determined by tuning the 3D position of the nuclei of the individual confocal pictures.

RESULTS

BrdU Incorporation Assay

The results of the cytotoxicity experiments with doxorubicin, CAELYX, and the albumin and transferrin conjugates in the LXFL 529 lung carcinoma cell line are shown in Fig. 2 (compounds were tested in the range from 0.01 to 10 μM). Doxorubicin has a strong inhibitory effect on DNA synthesis with an IC_{50} value of around 0.04 μM. The acid-sensitive conjugates A-DOXO-HYD and T-DOXO-HYD are also active in this cell line with comparable IC_{50} values for both derivatives (0.3 μM for A-DOXO-HYD, 0.4 μM for T-DOXO-HYD); CAELYX showed a significantly lower inhibitory efficacy (IC_{50} value ~3.0 μM). The stable albumin conjugate A-DOXO-MBS does not inhibit DNA-synthesis at the concentrations tested.

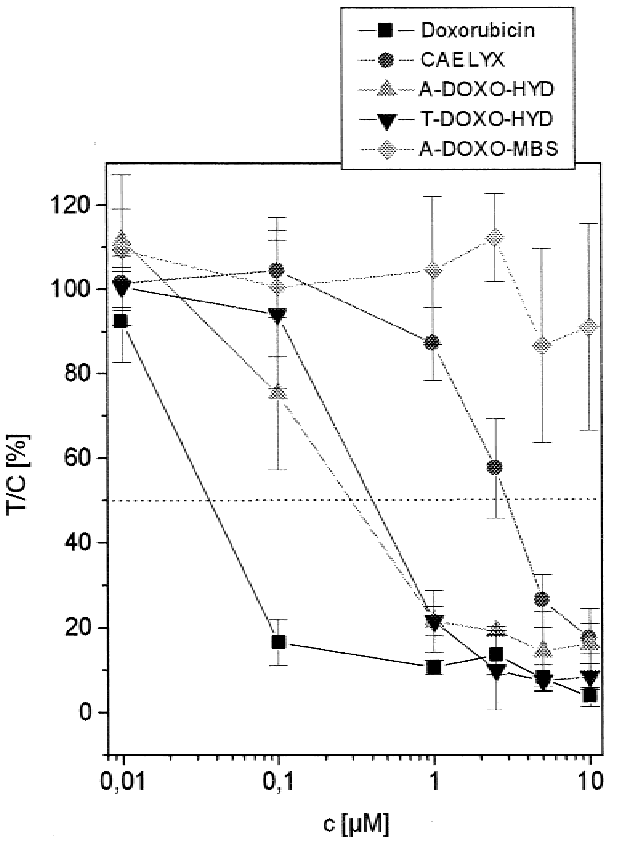

Fig. 2. Influence of free doxorubicin, CAELYX, A-DOXO-HYD, T-DOXO-HYD and A-DOXO-MBS (IC_{50} not reached) on DNA synthesis in the LXFL 529 lung carcinoma cell line.

CLSM Double Fluorescence Studies with Doxorubicin and Doxorubicin Derivatives: Organelle-Specific Staining of Lysosomes, Mitochondria, and Golgi Apparatus

To characterize the fluorescent properties of doxorubicin and the doxorubicin formulations prior to incubation with the tumor cells, fluorescence spectra of a 3 μM solution of doxorubicin, T-DOXO-HYD, A-DOXO-HYD, A-DOXO-MBS, and CAELYX were recorded which revealed that the relative intensity of the maximum fluorescence emission at 555–560 nm for free doxorubicin is approximately three- to fourfold higher compared to the conjugates, and sixfold higher compared to CAELYX. This difference in the fluorescent properties of the drug formulations was, in part, compensated in the CLSM studies by incubating the cells with a higher concentration of the doxorubicin formulations (2 μM) compared to free doxorubicin (1 μM). When doxorubicin or the doxorubicin formulations were incubated with one or five equivalents of human serum albumin, only marginal changes (<10%) were observed in the fluorescence spectra.

When CAELYX was incubated for 24 h at 37°C with phosphate buffer (3 μM) or 10% FCS, the relative intensity of the maximum fluorescence emission at 555–560 nm increased by approximately 30–40% over the initial value, which corresponds to 5–10% leakage of doxorubicin from the liposome when compared with the relative intensity of the maximum fluorescence emission at 555–560 nm of a 3 μM solution of free doxorubicin. Incubation studies with calf thymus DNA resulted in pronounced quenching (>90%) of the intrinsic fluorescence of the anthracycline chromophore in the case of doxorubicin. Quenching for the acid-sensitive protein conjugates was lower (T-DOXO-HYD [~50%], A-DOXO-HYD [~30%]), whereas only marginal quenching was observed for A-DOXO-MBS and CAELYX (<10%). These results are in accordance with those obtained in an analogous study with polyethylene glycol doxorubicin conjugates (15) and indicate that the anthracycline moiety attached to the protein through a hydrazone linker is accessible for interactions with DNA.

To investigate and compare the cellular uptake as well as the intracellular distribution of A-DOXO-HYD, A-DOXO-MBS, T-DOXO-HYD, CAELYX, and free doxorubicin, LXFL 529 lung carcinoma cells were incubated with the drug formulations for 4 and 24 h, respectively, followed by a 15 min incubation with the respective fluorescence organelle-specific marker. Because of the observation in earlier experiments that fixation of the cells resulted in a falsification of the fluorescence staining, we used living cells in our double-labeling experiments.

In a first series of experiments, LXFL 529 cells were incubated with the doxorubicin derivatives for 4 h, followed by incubation with the lysosomal marker. The results of these studies are shown in Fig. 3A–E for all compounds as a single layer through the middle of the cells. Doxorubicin is primarily localized in the cell nucleus after this time (Fig. 3A), which is in accord with the literature data (16,17). In contrast, when the cells were incubated with A-DOXO-HYD, A-DOXO-MBS, or T-DOXO-HYD, no or only marginal fluorescence was detected in the nucleus and was mainly observed in the cytoplasm. The fluorescence intensity observed with CAELYX after 4 h was lower compared to the other compounds (Fig. 3E). As shown in Fig. 3A–E, hardly any fluorescence resulting from doxorubicin is detected in the lysosomes with the exception of tumor cells incubated with doxorubicin, where some accumulation is observed. Double-labeling experiments with LysoTracker Red after 24 h revealed that doxorubicin from the derivatives did not accumulate to a much greater extent in these organelles (data not shown).

In a next set of experiments, we wanted to determine which intracellular compartments were the major sites of doxorubicin accumulation after 24 h for the different compounds. Thus, we performed double-labeling experiments with MitoTracker Red and the Golgi marker. The CLSM images are shown in Fig. 4A–E (MitoTracker Red) and Fig. 5A–E (Golgi marker); a representative single layer showing the fluorescence of doxorubicin and of the organelle marker as well as a pseudo-3D animation highlighting colocalization is shown from top to bottom.

After a 24 h incubation with free doxorubicin, fluorescence is now also observed in the cytoplasm of the LXFL 529 cells, and the double-labeling experiments show that a part of this fluorescence is associated with mitochondria as well as the Golgi apparatus.

The doxorubicin protein conjugates A-DOXO-HYD, T-DOXO-HYD, and A-DOXO-MBS display a very similar cellular distribution pattern with the major fluorescence seen in the cytoplasm (Fig. 4B–D, Fig. 5B–D). After 24 h, fluorescence was also detected in the nucleus for A-DOXO-HYD; in contrast, hardly any fluorescence was discernible in the nucleus of the tumor cells that were incubated with T-DOXO-HYD or A-DOXO-MBS (Figs. 4 and 5C and D). Double-labeling experiments show that doxorubicin from the conjugates is localized in the mitochondria as well as in the Golgi apparatus. This feature is clearly seen when comparing the individual pictures for the conjugates and organelle markers with the colocalization pictures showing the overlap of the two fluorescence signals.

Fluorescence in LXFL 529 cells that were incubated with CAELYX is seen in the nucleus and, in part, in the cytoplasm. Double-labeling experiments indicate that the cytoplasmic compartment contains rather mitochondria and not the Golgi apparatus.

DISCUSSION

CLSM does not allow one to distinguish between protein-bound or encapsulated doxorubicin and intracellulary liberated doxorubicin. The fluorescence intensity of doxorubicin is dependent on the microenvironment within the cell and physical parameters such as concentration and pH value (18). Above all, pronounced quenching is observed when doxorubicin intercalates with DNA (19–21). Taking this into consideration, confocal fluorescence microscopy does not give a quantitative description of the intracellular distribution of doxorubicin formulations, but has been shown to be a useful noninvasive technique for identifying principal sites of drug localization (16,17,21).

A first objective of the present work was thus to assess any major differences regarding the intracellular distribution after incubation of lung cancer cells with free doxorubicin, doxorubicin protein conjugates, and a liposomal formulation of doxorubicin. A second objective was to investigate whether doxorubicin accumulated in lysosomes, the Golgi apparatus,

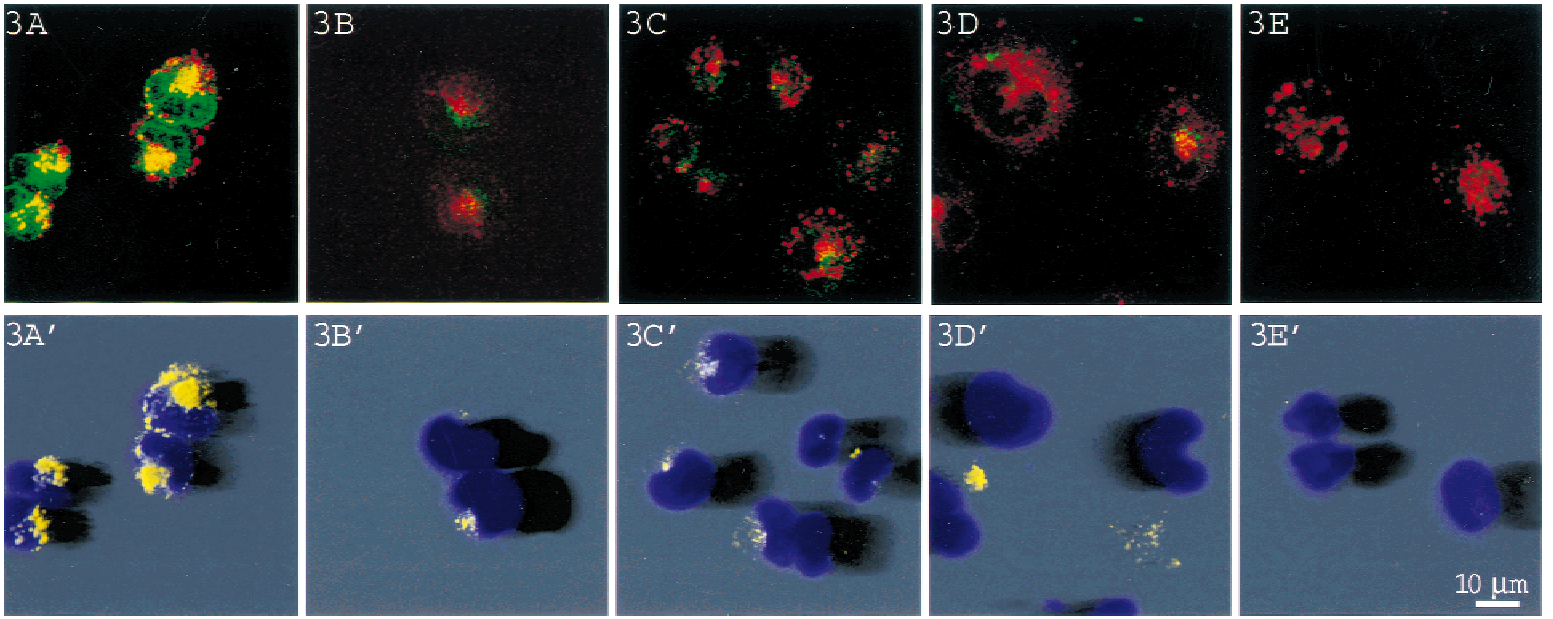

Fig. 3. CLSM images depicting the intracellular distribution of doxorubicin (A; green), A-DOXO-HYD (B; green), A-DOXO-MBS (C; green), T-DOXO-HYD (D; green), CAELYX (E; green), and the lysosome marker (A, B, C, D, E; red) in LXFL 529 cells after 4 h. Colocalization of doxorubicin and derivatives with lysosomes (yellow) and the cell nuclei (blue) is shown in A′, B′, C′, D′, and E′. Pictures A, B, C, D, and E are single optical sections taken in the middle of the cells; pictures A′, B′,.C′, D′, and E′ represent 3D reconstructions.

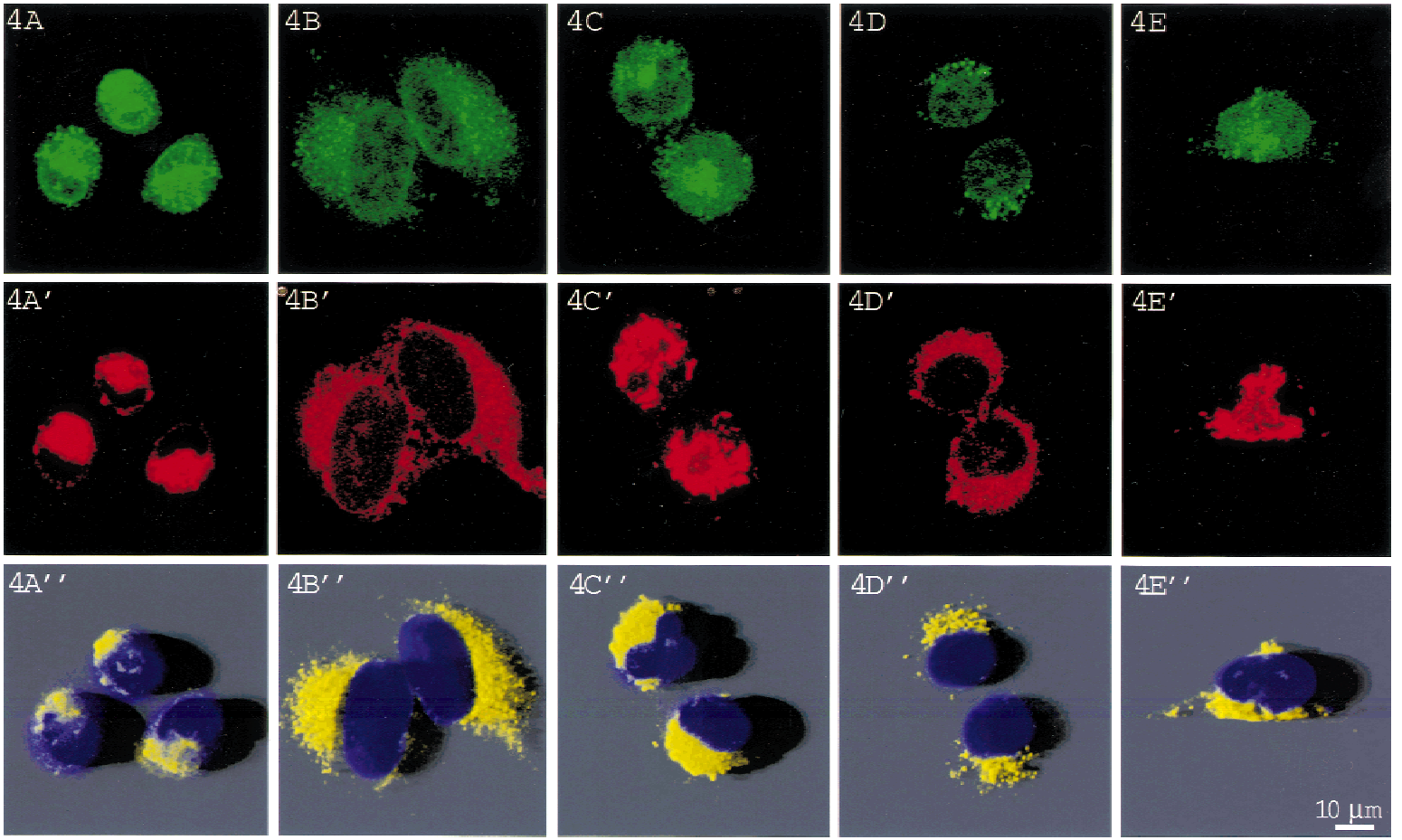

Fig. 4. CLSM images depicting the intracellular distribution of doxorubicin (A; green), A-DOXO-HYD (B; green), A-DOXO-MBS (C; green), T-DOXO-HYD (D; green), CAELYX (E; green), and the mitochondrium marker (A′, B′, C′, D′, E′; red) in LXFL 529 cells after 24 h. Colocalization of doxorubicin and derivatives with the mitochondria (yellow) and the cell nuclei (blue) is shown in A″, B″, C″, D″, and E″. Pictures A, A′, B, B′, C, C′, D, D′, E, and E′ are single optical sections taken in the middle of the cells; pictures A″, B″, C″, D″, and E″ represent 3D reconstructions.

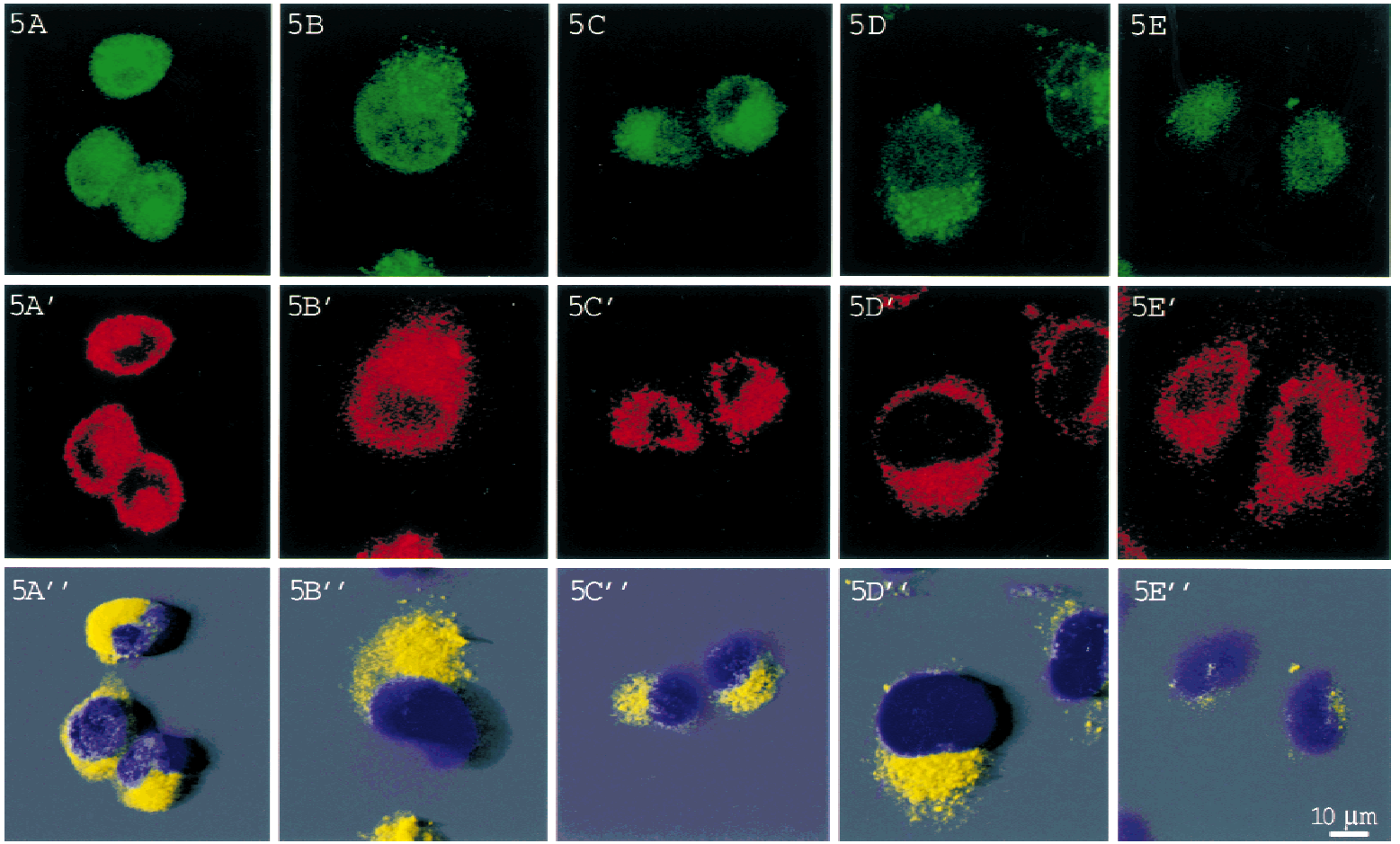

Fig. 5. CLSM images depicting the intracellular distribution of doxorubicin (A; green), A-DOXO-HYD (B; green), A-DOXO-MBS (C; green), T-DOXO-HYD (D; green), CAELYX (E; green), and the Golgi marker (A′, B′, C′, D′, E′; red) in LXFL 529 cells after 24 h. Colocalization of doxorubicin and derivatives with the Golgi apparatus (yellow) and the cell nuclei (blue) is shown in A″, B″, C″, D″, and E″. Pictures A, A′, B, B′, C, C′, D, D′, E, and E′ are single optical sections taken in the middle of the cells; pictures A″, B″, C″, D″, and E″ represent 3D reconstructions.

or mitochondria with the aid of double-labeling experiments. Emphasis was laid on these organelles because (a) lysosomes and the Golgi apparatus are important organelles during endocytosis and vesicle trafficking (22), and (b) cardiotoxicity of doxorubicin appears to be associated with the accumulation of this drug in the mitochondria of heart muscle cells (23,24).

Double-labeling experiments with a lysosome marker show that doxorubicin does not accumulate in these organelles when lung carcinoma cells are exposed to free doxorubicin or the doxorubicin derivatives. This result indicates that the concentrations of doxorubicin in lysosomes are too low to be detected by colocalization with the LysoTracker, either because the doxorubicin protein conjugates, CAELYX, or intracellularly released doxorubicin from these formulations are not transported to lysosomes, or because once released, doxorubicin diffuses rapidly from the lysosomes into the cytoplasm or because lysosomes fuse with other organelles, thus trafficking the doxorubicin compounds to new intracellular compartments.

Key differences between doxorubicin and the doxorubicin protein conjugates are the initial intracellular sites of accumulation and the shift between nucleus and cytoplasm with time: doxorubicin is primarily localized in the nucleus during the first hours of incubation (after 1 h it is almost solely confined to the nucleus when incubated with 1 μM of doxorubicin [data not shown]) with fluorescence also seen in the cytoplasm after 4 h. In a related study by Lopes de Menezes et al. (21), who incubated a B lymphoma cell suspension for 1 h with doxorubicin, doxorubicin fluorescence was observed in the nucleus as well as in the cytoplasm using confocal microscopy. In addition, subcellular fractionation showed that after a 1 h incubation with doxorubicin at 10°C, approximately 20% of doxorubicin was found in the cell nucleus and approximately 40% in the mitochondria as shown by HPLC.

In contrast to the results obtained with free doxorubicin, cells incubated with the doxorubicin protein conjugates are practically devoid of fluorescence in the nucleus after 4 h in our study. Because we have shown that the stable conjugate A-DOXO-MBS shows marginal quenching and the acid-sensitive transferrin and albumin conjugate demonstrate quenching to a lesser extent than free doxorubicin when incubated with DNA, we can conclude that less doxorubicin is delivered to the cell nucleus when LXFL 529 cells are incubated with the doxorubicin protein conjugates.

After 24 h, considerable fluorescence is seen in the cytoplasm of cells incubated with either doxorubicin or the protein conjugates. In addition, some fluorescence is now also observed in the nucleus of cells treated with the conjugates, although of very weak intensity in the case of A-DOXO-MBS and T-DOXO-HYD (see Fig. 4C,D and Fig. 5C,D). When LXFL 529 cells were incubated with CAELYX for 4 and 24 h, the major amount of doxorubicin fluorescence is observed in the nucleus.

Our double-labeling experiments indicate that doxorubicin that is detected in the cytoplasm is localized in mitochondria as well as in the Golgi apparatus. The extent of colocalization is particularly pronounced in the incubation studies with the doxorubicin conjugates A-DOXO-HYD, T-DOXO-HYD, and A-DOXO-MBS (see Fig. 4 and Fig. 5B–D). Accumulation of the drug protein conjugates in the Golgi apparatus would be expected considering that the Golgi apparatus and the trans-Golgi network play a pivotal role in the sorting of vesicles that enter and leave the cell (22). The other sites of doxorubicin accumulation are the mitochondria. Several studies have shown that doxorubicin impairs the function of heart mitochondria by interacting with the negatively charged phospholipid, cardiolipin, by inhibiting mitochondrial enzymes or by lipid peroxidation, leading to an overall inhibition of cell respiration (23,24). Moreover, Nicolay et al. demonstrated by fluorescence microscopy that heart mitochondria and the nucleus are the predominant sites of doxorubicin localization (24). Our results would now suggest that the mitochondria of lung carcinoma cells are also sites of drug accumulation by which free doxorubicin as well as doxorubicin from the investigated drug formulations exert their cytotoxicity: Specific localization of doxorubicin in mitochondria is especially pronounced for the protein doxorubicin conjugates and is also seen when LXFL 529 cells are exposed to free doxorubicin for a longer period. Considering the fact that only weak fluorescence was observed in the cell nucleus when the cells were exposed to the doxorubicin protein conjugates, we can tentatively suggest that the inhibition of mitochondrial function is an important factor by which acid-sensitive transferrin and albumin conjugates of doxorubicin kill tumor cells. Whether doxorubicin additionally accumulates in other organelles such as the endoplasmic reticulum cannot be ruled out by our studies, however (double labeling experiments were not carried out with a marker for the endoplasmatic reticulum because a unique marker for this cellular compartment is not commercially available).

A surprising result from our investigation is that the intracellular fluorescence pattern of the three doxorubicin conjugates is, on the whole, quite similar despite the fact that the stable amide conjugate A-DOXO-MBS does not exhibit cytotoxicity in contrast to the acid-sensitive conjugates A-DOXO-HYD and T-DOXO-HYD (see Fig. 2). This result is a first indication that the conjugates are taken up by LXFL 529 cells and trafficked intracellularly in a similar manner irrespective of the chemical bond between the drug and the protein. Furthermore, there is no pronounced difference between the acid-sensitive transferrin and albumin conjugates T-DOXO-HYD and A-DOXO-HYD with respect to cellular sublocalization and cytotoxicity.

Our experiments do not allow us to define the endocytotic pathways of the doxorubicin protein conjugates in detail. The following observations, however, suggest that endocytosis of the transferrin conjugate by the transferrin receptor may not necessarily be the dominant factor by which such conjugates exert their cytotoxicity.

We have previously noted that extensive in vitro and in vivo studies with transferrin and albumin drug conjugates did not reveal a significant difference between the two proteins as potential drug carriers (4,5,25,26). An approximate estimation of the ratio of the number of doxorubicin transferrin conjugates to the number of transferrin receptors expressed on tumor cells (approximately $0.5–2 \times 10^6$) (27) reveals a ratio of around $10^5–10^6$:1 at the IC_{50} values of doxorubicin protein conjugates in cell culture systems (0.1–1.0 μM). This indicates that the contribution of the transferrin receptor might be small when other endocytotic pathways in tumor cells are dominant, especially when cells are exposed to relatively high drug concentrations (1.0–2.0 μM). It should be added that the IC_{50} values of transferrin and albumin conjugates with chlorambucil were nearly identical in MOLT4 leukemia and

MCF7 breast carcinoma cells despite the fact that the transferrin receptor was expressed on these tumor cells (25,26). In addition, analogously constructed doxorubicin conjugates with polyethylene glycol of molecular weight 20,000 and 70,000 Da showed very similar in vitro activity compared to the corresponding transferrin conjugates (15). Fluorescence microscopy studies with doxorubicin polyethylene glycol conjugates with LXFL 529 cells also demonstrated that the nucleus was practically devoid of any fluorescence (15).

We would like to point out, however, that the drug loading ratio in our conjugates is very low (1.0–1.5). The role of the transferrin receptor or other tumor-associated receptors will certainly be of great importance when large amounts of drugs are incorporated into the internalizing carrier, such as is the case with liposomes carrying targeting moieties, for instance (28).

Whether cellular uptake of CAELYX takes place by endocytosis is not clear from our studies. A number of studies have indicated that the dominant mechanism for cellular uptake of liposomal formulations is drug leakage from the liposome in the cell culture medium and subsequent diffusion of free drug into the cell (29,30). Our incubation studies with CAELYX in physiological buffer or 10% FCS show that slow drug leakage occurs over 24 h. This observation, as well as the weak intracellular fluorescence intensity detected after incubation of LXFL 529 cells with CAELYX, suggests that endocytosis is not the major mechanism for cellular uptake. Recent investigations with a very similar pegylated liposomal formulation of doxorubicin (DXR-SL) have also revealed a much weaker intracellular fluorescence intensity when B lymphoma cells were incubated with DXR-SL compared to free doxorubicin (21). In addition, the cytotoxicity of DXR-SL could be significantly reduced (greater than fivefold) in the presence of a cation exchange resin (Dowex), which removes liberated doxorubicin from the cell culture medium. The IC_{50} value of DXR-SL was approximately 25-fold lower than that for free doxorubicin (after an incubation time of 24 h with B lymphoma cells) compared to a 75-fold decrease noted in our study.

Further experiments are warranted in order to obtain a detailed picture of the precise endocytotic pathways for different drug delivery systems on the cellular level.

In summary, our in vitro studies in LXF529 lung carcinoma cells show that following drug exposure:

1. Free doxorubicin and doxorubicin from the liposomal doxorubicin (CEALYX) is initially localized in the cell nucleus and additionally observed in the Golgi apparatus and mitochondria with time.
2. Predominant sites of accumulation for doxorubicin transferrin and albumin conjugates are the Golgi apparatus and mitochondria.
3. The cellular distribution pattern and cytotoxicity of acid-sensitive transferrin and albumin conjugates are very similar.
4. Incorporating a stable amide bond between doxorubicin and albumin does not prevent cellular uptake of the conjugate but leads to a dramatic loss of cytotoxicity.
5. Inhibitory effects decrease in the order doxorubicin > acid-sensitive doxorubicin transferrin and albumin conjugates > CAELYX >> non-acid-sensitive doxorubicin albumin conjugate.

ACKNOWLEDGMENTS

This work has been supported by the Dr. Mildred Scheel Stiftung der Deutschen Krebshilfe, FRG and the Fördergesellschaft der Klinik für Tumorbiologie, Germany.

REFERENCES

1. Y. Takakura and M. Hashida. Macromolecular drug carrier systems in cancer chemotherapy: macromolecular prodrugs. *Crit. Rev. Oncol. Hematol.* **18**:207–231 (1994).
2. G. Gregoriadis (ed.). *Liposomes as Drug Carriers: Recent Trends and Progress,* John Wiley, Chichester, 1988.
3. H. Maeda and Y. Matsumura. Tumoritropic and lymphotropic principles of macromolecular prodrugs. *Crit. Rev. Ther. Drug Carrier Syst.* **6**:193–210 (1989).
4. F. Kratz, U. Beyer, T. Roth, N. Tarasova, P. Collery, F. Lechenault, A. Cazabat, P. Schumacher, C. Unger, and U. Falken. Transferrin conjugates of doxorubicin: Synthesis, characterization, cellular uptake, and in vitro efficacy. *J. Pharm. Sci.* **87**:338–346 (1998).
5. F. Kratz, U. Beyer, P. Collery, F. Lechenault, A. Cazabat, P. Schumacher, U. Falken, and C. Unger. Preparation, characterization, and in vitro efficacy of albumin conjugates of doxorubicin. *Biol. Pharm. Bull.* **21**:56–61 (1998).
6. F. Kratz, U. Beyer, and M. T. Schütte. Drug-polymer conjugates containing acid-cleavable bonds, *Crit. Rev. Ther. Drug Carrier Syst.* **16**:245–288 (1999).
7. J. Drevs, I. Hofmann, D. Marmé, C. Unger, and F. Kratz. In vivo and in vitro efficacy of an acid-sensitive albumin conjugate of adriamycin compared to the parent compound in murine renal cell carcinoma. *Drug Deliv.* **6**:1–7 (1999).
8. F. Kratz, T. Roth, I. Fichtner, H. H. Fiebig, and C. Unger: Development of antitumor protein and polymer conjugates using in vitro and in vivo human tumor xenograft models. In H. H. Fiebig and A. M. Burger (eds.), *Contributions to Oncology, Vol. 54, Relevance of Tumor Models for Anticancer Drug Development,* 1999, pp. 389–395.
9. T. M. Allen. Liposomes. Opportunities in drug delivery. *Drugs* **54**:8–14 (1997).
10. A. Gordon, J. Fleagle, D. Guthrie, D. Parrkin, M. Gore, A. Lacave, and D. Mutch. Interim analysis of a phase II randomized trial of Doxil/Caelyx (D) versus topotecan (T) in the treatment of patients with relapsed ovarian cancer. *Proc. Am. Soc. Oncol.* **19**: 380a (2000).
11. D. Shotton and N. White. Confocal scanning microscopy: three dimensional biological imaging. *Trends Biochem. Sci.* **14**:435–439 (1989).
12. R. C. Gonzales and P. Wintz. *Digital Image Processing,* Addison-Wesley, Reading, MA, 1987.
13. B. Rothen-Rutishauser, S. D. Krämer, A. Braun, M. Günthert, and H. Wunderli-Allenspach. MDCK cell cultures as an epithelial in vitro model: Cytoskeleton and tight junctions as indicators for the definition of age-related stages by confocal microscopy. *Pharm. Res.* **15**:964–971 (1998).
14. F. Kratz, R. Müller-Driver, I. Hofmann, J. Drevs, and C. Unger. A novel macromolecular prodrug concept exploiting endogenous serum albumin as a drug carrier for cancer chemotherapy. *J. Med. Chem.* **43**:1253–1256 (2000).
15. P. A. Rodrigues, P. Schumacher, U. Beyer, T. Roth, H. H. Fiebig, C. Unger, D. Paper, L. Messori, P. Orioli, R. Mülhaupt, and F. Kratz. Acid-sensitive polyethylene glycol conjugates of doxorubicin: preparation, in vitro efficacy and cellular uptake. *Bioorg. Med. Chem.* **7**:2517–2524 (1999).
16. H. M. Coley, W. B. Amoa, P. R. Twentyman, and P. Workman. Examination by laser scanning confocal fluorescence imaging microscopy of the subcellular localisation of anthracyclines in parent and multidrug resistant cell lines. *Br. J. Cancer* **67**:1316–1323 (1993).
17. A. Krishan, K. S. Sridhar, E. Davilla, C. Vogel, and W. Sternheim. Patterns of anthracycline retention modulation in human tumor cells. *Cytometry* **8**:306–314 (1987).
18. K. K. Karukstis, E. H. Z. Thompson, J. A. Whiles, and R. J.

Rosenfeld. Deciphering the fluorescence of daunomycin and doxorubicin. *Biophys.Chem.* **73**:249–263 (1998).
19. J. B. Chaires, N. Dattagupta, and D. M. Crothers. Studies on the interaction of anthracycline antibiotics and deoxyribonucleic acid: Equilibrium binding studies on interaction of daunomycin with deoxyribonucleic acid. *Biochemistry* **21**:3933–3940 (1982).
20. K. Barabas, J. A. Sizensky, and W. P. Faulk. Transferrin conjugates of adriamycin are cytotoxic without intercalating nuclear DNA. *J. Biol. Chem.* **267**:9437–9442 (1992).
21. D. E. Lopes de Menezes, M. J. Kirchmeister, J. Gagne, L. M. Pilarski, and T. M. Allen. Cellular trafficking and cytotoxicity of anti-CD19-targeted liposomal doxorubicin in B lymphoma cells, *J. Liposome Res.* **9**:199–228 (1999).
22. S. Mukherjee, R. N. Grosh, and F. R. Maxfield. Endocytosis. *Physiol. Rev.* **77**:759–803 (1997).
23. K. Nicolay and B. De Kruijff. Effects of adriamycin on respiratory chain activities in mitochondria from rat liver, rat heart and bovine heart. Evidence for preferential inhibition of complex III and IV. *Biochim. Biophys. Acta* **892**:320–330 (1987).
24. K. Nicolay, J. J. Fok, W. Voorhout, J. A. Post, and B. De Kruijff. Cytofluorescence detection of adriamycin-mitochondria interactions in isolated, perfused rat heart. *Biochim. Biophys. Acta* **887**: 35–41 (1986).
25. U. Beyer, T. Roth, A. Unold, P. Schumacher, G. Maier, A. W. Frahm, H. H. Fiebig, C. Unger, and F. Kratz. Transferrin conjugates of chlorambucil: Synthesis, in vitro efficacy and structure-activity-relationship. *J. Med. Chem.* **41**:2701–2708 (1998).
26. F. Kratz, U. Beyer, T. Roth, M. T. Schütte, A. Unold., H. H. Fiebig, and C. Unger. Albumin conjugates of the anticancer drug chlorambucil: Synthesis, characterization and in vitro efficacy. *Arch. Pharm., Pharm. Med. Chem.* **331**:47–53 (1998).
27. Brock, J. H. Transferrins. In P. M. Harrison (ed.), *Metalloproteins, Part 2: Metal Proteins with Non-redox Roles,* Verlag Chemie, Weinheim, 1985, pp. 183–263.
28. T. M. Allen, E. Brandeis, C. B. Hansen, G. Y. Kao, and S. Zalipsky. A new strategy for attachment of antibodies to sterically stabilized liposomes resulting in efficient targeting to cancer cells. *Biochim. Biophys. Acta* **123**:99–108 (1995).
29. D. Papahadjopoulos, T. M. Allen, A. Gabizon, A. Mayhew, E. Matthay, S. K. Huang, K. D. Lee, M. C. Woodle, D. D. Lasic, C. Redemann, and F. J. Martin. Sterically stabilized liposomes: improvements in pharmacokinetics and antitumor therapeutic efficacy. *Proc. Natl. Acad. Sci. USA* **88**:11460–11464 (1991).
30. N. Z. Wu, R. D. Braun, M. H. Gaber, G. M. Lim, E. T. Ong, S. Shan, D. Papahadjopoulos, and W. Dewhirst. Simultaneous measurement of liposome extravasation and content release in tumors. *Microcirculation* **4**:83–101 (1997).